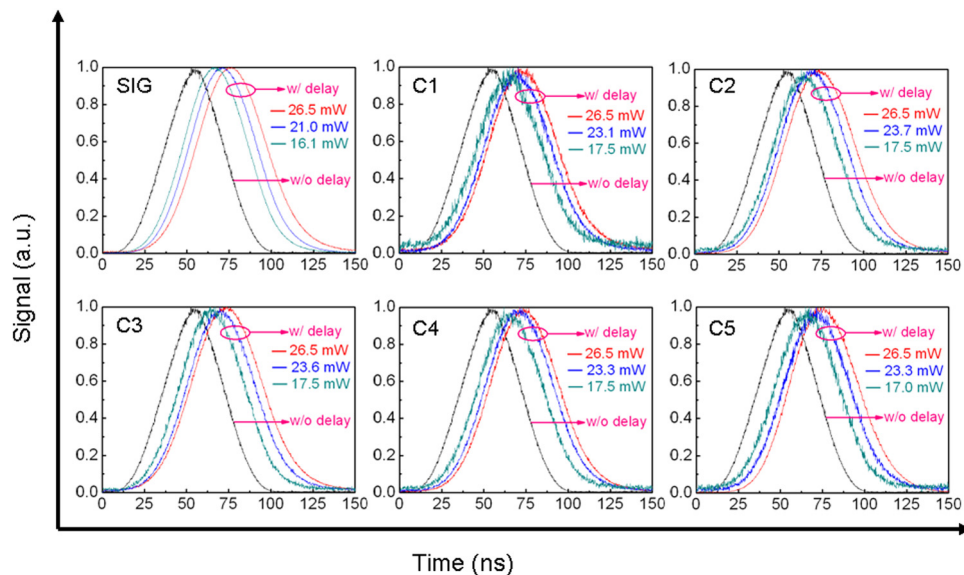


Generation of Multichannel Delayed Pulses by Four-Wave-Mixing-Assisted Stimulated Brillouin Scattering Slow-Light System

Volume 4, Number 4, August 2012

Liang Wang, Student Member, IEEE
Yimin Chen, Student Member, IEEE
Hon Ki Tsang, Senior Member, IEEE
Chester Shu, Senior Member, IEEE



DOI: 10.1109/JPHOT.2012.2207097
1943-0655/\$31.00 ©2012 IEEE

Generation of Multichannel Delayed Pulses by Four-Wave-Mixing-Assisted Stimulated Brillouin Scattering Slow-Light System

Liang Wang, *Student Member, IEEE*, Yimin Chen, *Student Member, IEEE*,
Hon Ki Tsang, *Senior Member, IEEE*, and Chester Shu, *Senior Member, IEEE*

Department of Electronic Engineering and Center for Advanced Research in Photonics,
The Chinese University of Hong Kong, Shatin, Hong Kong

DOI: 10.1109/JPHOT.2012.2207097
1943-0655/\$31.00 ©2012 IEEE

Manuscript received May 31, 2012; revised June 27, 2012; accepted June 27, 2012. Date of publication July 5, 2012; date of current version July 16, 2012. This work was supported by the Research Grants Council of Hong Kong (Project CUHK 416509). Corresponding author: L. Wang (e-mail: lwang@ee.cuhk.edu.hk).

Abstract: We demonstrate a technique to simultaneously generate multiple delayed signals through four-wave mixing (FWM) wavelength multicasting in a single-pump stimulated Brillouin scattering (SBS)-based slow-light system. The signal delay is achieved with an SBS pump while, at the same time, the delay is transferred to six other channels by three FWM pumps employed for wavelength multicasting. The delay performances of all output channels are analyzed. Relationship of the delay between the original signal and the multicast outputs is investigated and verified experimentally.

Index Terms: Four-wave mixing, stimulated Brillouin scattering slow light, wavelength multicasting.

1. Introduction

Slow light in nonlinear media has attracted considerable interest because of its numerous applications, such as variable true time delay and optical information processing [1]. In early slow-light research, several commonly used techniques are electromagnetically induced transparency (EIT) [2], coherent population oscillations (CPOs) [3], and waveguiding in photonic crystals [4]. In 2005, Okawachi *et al.* [5] and Song *et al.* [6] achieved slow light in optical fibers via stimulated Brillouin scattering (SBS). Using fibers to achieve slow light offers the advantages of room-temperature operation and device compatibility with existing fiber systems. Later, by exploiting pump spectral broadening techniques [7]–[9], SBS slow light has been used to support \sim GHz signal bandwidth. The technique resulted in many demonstrations on the delay of \sim Gb/s communication data [10]–[15]. At the same time, slow-light-induced signal distortion has been intensively studied, and plenty of methods have been applied to minimize the distortion [16]–[21]. Apart from communications, SBS slow light has also been applied to other areas such as fiber sensing [22], [23].

Owing to the tight requirement of spectral alignment between the SBS pump and the signal, most of the published works are for the case where one SBS pump is used to delay a single channel. Hence, only one delayed channel is obtained. If multiple delayed signals can be simultaneously generated with a single SBS pump, the potential for multichannel signal processing can be unveiled. Examples of parallel processing with multiple pulsed or data outputs are multichannel synchronization, multichannel time-division multiplexing, and multichannel regeneration. A common

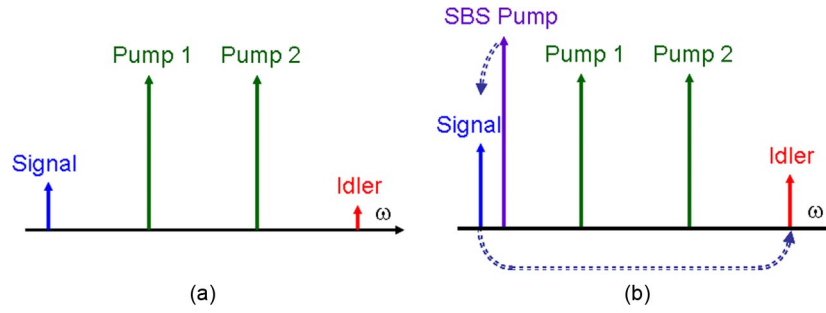


Fig. 1. Spectral assignment in (a) conventional nondegenerate FWM; (b) nondegenerate FWM with slow light transferred from signal to idler.

approach of generating multichannel signals is by four-wave mixing (FWM) wavelength multicast through which the information carried by a single signal is copied to different wavelengths [24]–[27]. In this paper, we demonstrate simultaneous generation of multichannel delayed pulses by using FWM in a single-pump SBS slow-light system. The SBS delay of the signal is successfully transferred to six channels through FWM wavelength multicast. It is worth mentioning that FWM has previously been used to perform single-channel slow-light conversion [28]. However, there was no report on analyzing the relationship between the delay of the idler and that of the original signal. Here, we demonstrate simultaneous multichannel slow-light conversion using a single SBS pump. Both theoretical and experimental investigations of the delay performance of the six output channels have been carried out. The relationship of the time delay between the original signal and that of the multicast outputs is analyzed.

2. Principle

The spectral plot for a conventional nondegenerate FWM process is illustrated in Fig. 1(a). The index grating caused by the beating between the signal and pump 1 scatters pump 2 to generate an idler. If the pumps remain undepleted during the FWM process, the power of the converted idler can be expressed as [29], [30]

$$P_i(L) = \eta(\kappa)\gamma^2 L_{\text{eff}}^2 P_1 P_2 P_s e^{-\alpha L}. \quad (1)$$

Here, γ is the nonlinear coefficient of the fiber; P_1 , P_2 , and P_s are the power of pump 1, pump 2, and signal, respectively; L is the fiber length; α is the attenuation coefficient; $L_{\text{eff}} = [1 - \exp(-\alpha L)]/\alpha$ is the effective fiber length; $\eta(\kappa)$ is the FWM efficiency; and $\kappa = \Delta k + \gamma(P_1 + P_2)$ is defined as the effective phase mismatch with Δk representing the linear phase mismatch. When the phase matching is perfect ($\kappa = 0$), $\eta(\kappa)$ reaches its maximum value. For SBS to take place, the signal and the SBS pump should counter-propagate in the fiber where the signal is amplified and delayed by the slow-light effect. The complex Brillouin gain coefficient is [5], [30]

$$g_b(\delta) = \frac{g_0}{1 - i\delta} = \frac{g_0}{1 - j \frac{(\omega_p - \omega_s - \Omega_B)}{\Gamma_B/2}} \quad (2)$$

in which g_0 is the peak gain, ω_p and ω_s are the frequencies of the SBS pump and signal, Ω_B is the Brillouin frequency shift, Γ_B is the gain bandwidth, and $\delta = (\omega_p - \omega_s - \Omega_B)/(\Gamma_B/2)$ is the normalized frequency detuning of the signal from the Stokes wave. The real part of the complex Brillouin gain coefficient $\text{Re}(g_b)$ is related to the gain of the signal, causing it to grow exponentially if pump depletion is neglected. Thus,

$$P_s(L) = P_s(0) e^{\text{Re}(g_b) P_p L_{\text{eff}} / A_{\text{eff}} - \alpha L} \quad (3)$$

where P_p is the SBS pump power, and A_{eff} is the fiber effective mode area. The imaginary part $\text{Im}(g_b)$ accounts for the slow-light effect, and the time delay is [30]

$$\Delta t = \Delta t_m \times \frac{1 - \delta^2}{(1 + \delta^2)^2} = \left(\frac{g_0 L P_p}{\Gamma_B A_{\text{eff}}} \right) \frac{1 - \delta^2}{(1 + \delta^2)^2} \quad (4)$$

where $\Delta t_m = g_0 L P_p / (\Gamma_B A_{\text{eff}})$ is the maximum delay time that occurs when the signal frequency is aligned to the Brillouin gain peak. Δt_m is only dependent on the maximum gain parameter $G_0 = g_0 L P_p / A_{\text{eff}}$ and the gain bandwidth Γ_B . We now consider the case where a counter-propagating SBS pump is introduced to delay the signal, as shown in Fig. 1(b). Owing to SBS–FWM interaction, the phase mismatch will become [31]

$$\kappa = \Delta k + \gamma(P_1 + P_2) - \text{Im}[g_b(\delta)]P_p \quad (5)$$

and the power of the idler will be

$$P_i(L) = \eta(\kappa) \gamma^2 L_{\text{eff}}^2 P_1 P_2 P_s e^{\text{Re}(g_b) P_p L_{\text{eff}} / A_{\text{eff}}} e^{-\alpha L}. \quad (6)$$

Equation (5) implies that the phase mismatch can be controlled by adjusting the frequency detuning δ [31]. Compared with the case without SBS described by (1), not only the signal power is increased but the FWM efficiency is also affected. As the idler power is proportional to the signal power, the SBS gain to the signal ($\text{Re}(g_b)$) will be completely transferred to the idler. Hence, the idler should experience the same SBS gain as that of the signal, although its net gain may differ due to the change in FWM efficiency. Furthermore, the phase change of the signal ($\text{Im}(g_b)$) caused by SBS should also be copied to the idler because FWM is a phase transparent process. Since both the real and imaginary parts of the complex Brillouin gain coefficient are transferred by the FWM process, the idler and the signal should have almost identical time delay. Therefore, when multiple pumps are introduced for FWM wavelength multicast in the presence of a single SBS pump for slow light, multiple copies of the delayed signal can be simultaneously produced. It is important to note that the SBS time delay transferred to the idlers depends only on the SBS gain parameter rather than on the net gain of the idlers, which is also determined by the FWM efficiency.

3. Experimental Setup

The experimental setup is shown in Fig. 2. The output of a tunable laser is split into two branches. The lower branch is amplified by an erbium-doped fiber amplifier (EDFA) and serves as the SBS pump. The amplified spontaneous emission (ASE) noise from the EDFA is filtered out by a bandpass filter (BPF). The upper branch is first modulated by an electro-optic intensity modulator (EOM-1) biased to suppress the optical carrier and driven at a frequency equal to the Brillouin frequency shift ($f_B = \Omega_B / 2\pi$). The optical spectrum after the modulation is depicted in Fig. 3(a). The carrier suppression ratio is over 23 dB. Next, a wave shaper is used as a narrow-band filter to select the longer wavelength sideband (1547.66 nm), as shown in Fig. 3(b). This sideband is then intensity modulated by EOM-2 to produce a 40-ns signal pulse. The signal passes through another EDFA and a variable optical attenuator (VOA) to facilitate control of its power. To introduce FWM, three optical pumps are provided from a wavelength-division multiplexing (WDM) transmitter. They are amplified by an EDFA to a total power of 130 mW and are combined with the signal through a 3-dB coupler. The three FWM pumps are set at unequally spaced wavelength of 1548.58, 1551.66, and 1557.58 nm to minimize crosstalk from pump beatings [27]. The signal together with the three pumps are directed to a 1-km highly nonlinear fiber (HNLf) where FWM takes place in the presence of the counter-propagating SBS pump. The HNLf has a nonlinear coefficient of $11 / (\text{W} \cdot \text{km})$, a dispersion coefficient of $-0.4 \text{ ps}/(\text{nm} \cdot \text{km})$, and a dispersion slope of $5.7 \times 10^{-3} \text{ ps}/(\text{nm}^2 \cdot \text{km})$ at $\sim 1550 \text{ nm}$. The Brillouin frequency shift and gain bandwidth of the HNLf are measured to be 9.71 GHz and 40 MHz, respectively. As the signal is slowed down by the SBS pump, its delay is

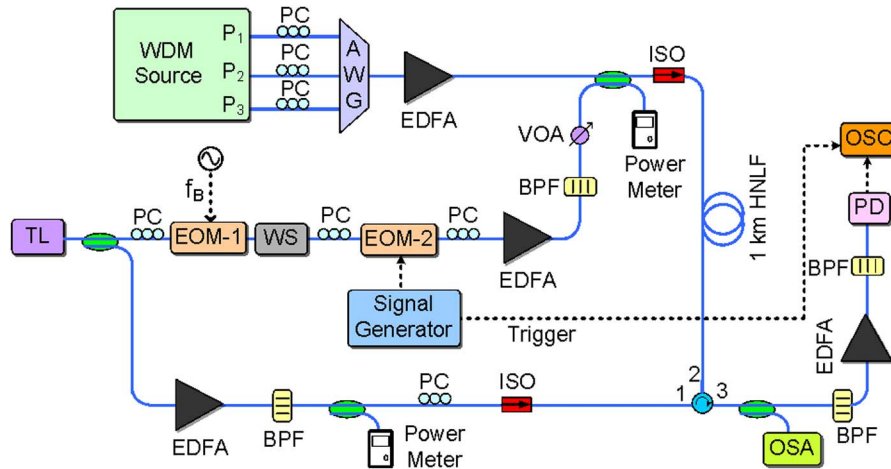


Fig. 2. Experimental setup for the generation of multichannel delayed signals. TL: tunable laser; AWG: arrayed waveguide grating; EOM: electro-optic intensity modulator; WS: wave shaper; EDFA: erbium-doped fiber amplifier; PC: polarization controller; VOA: variable optical attenuator; BPF: bandpass filter; HNLF: highly nonlinear fiber; ISO: isolator; OSA: optical spectrum analyzer; PD: photo-detector; OSC: oscilloscope.

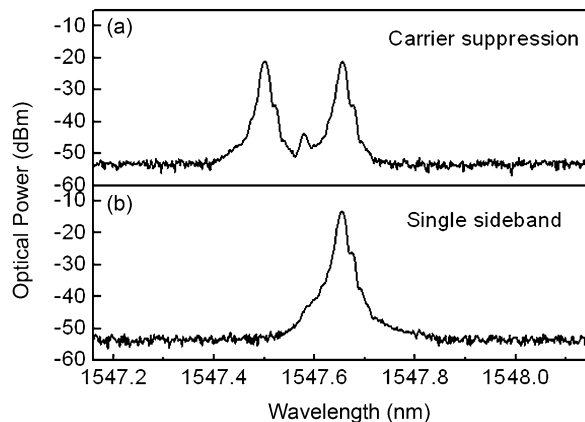


Fig. 3. Optical spectrum of (a) carrier suppressed modulated output; (b) filtered sideband at longer wavelength.

transferred to all the multicasting channels (converted idlers) through FWM. A 0.3-nm BFP is used at port 3 of the optical circulator to extract individual channels, which are then amplified and analyzed.

4. Results and Discussion

Fig. 4(a) plots the FWM spectrum (measured at port 3 of the optical circulator) when the signal power is intentionally reduced and the SBS pump is turned off. The FWM components are mainly caused by beatings among the three FWM pumps. After the SBS pump is turned on, the resultant spectrum is shown in Fig. 4(b). The signal is amplified and delayed by the SBS pump, while, at the same time, it is copied to six wavelengths from channel 1 to channel 6. The degenerate FWM between the signal and pump 1 generates channel 1. The index grating produced by the beating between the signal and pump 1 scatters pump 2 to generate channel 2 and channel 3 and scatters pump 3 to generate channel 4 and channel 5. Channel 6 is generated through scattering of the signal by the index grating originated from the beating of pump 1 and pump 2. The conversion

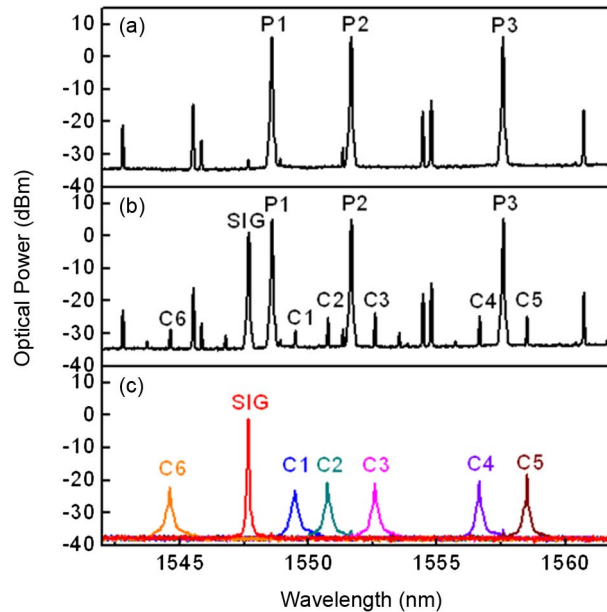


Fig. 4. Optical spectra showing (a) FWM without SBS pump; (b) FWM in the presence of a 26.5-mW SBS pump; (c) delayed signal and multicast outputs.

efficiencies from channel 1 to channel 6 are -30 dB, -25.22 dB, -24.48 dB, -25.66 dB, -25.75 dB, and -29.64 dB, respectively. The relatively low optical signal-to-noise ratio (OSNR) of the converted idlers observed in Fig. 4(b) may be caused by nonoptimized polarization states of the three FWM pumps and the finite spectral resolution (0.1 nm) of the optical spectrum analyzer. Another reason is that although the SBS gain of the signal should be transferred to the idlers, the power increase of the idlers are actually smaller because the SBS process also changes the FWM efficiency by increasing the phase mismatch. The phenomenon is currently under further investigation. To enhance the output OSNR, one may consider increasing the input signal power. However, the achievable maximum delay will be reduced because the signal gain will be saturated at a lower level [5]. A tradeoff should thus be adopted. Fig. 4(c) shows the spectra (measured just before the photo-detector) of the individually extracted channels including the signal by tuning the center wavelength of the BPF. Other higher order FWM components are not selected due to the low conversion efficiencies.

To investigate the performance of the time delay for each individual channel, we fix the center wavelength of the BPF to select one channel at a time. The time delay is measured at different SBS pump power levels. The results are presented in Fig. 5(a) and (b). For the signal itself, different time delays are obtained at different SBS pump power levels (shown as the red, blue, and green curves in Fig. 5(a)-SIG). The time delay grows linearly with the increase in the SBS pump power, as shown in Fig. 5(b)-SIG. The maximum time delay is ~ 20 ns and is achieved at 26.5-mW SBS pump power. At higher input pump power, the delay will not change much owing to gain saturation of the signal as well as saturation of the pump field caused by SBS generation of a Stokes field at the output fiber end [5]. It is noticed that the time delay is accompanied by a slight pulse broadening. From $-C5$, we can see clearly that all the converted channels are delayed, and the time delay is also related to the SBS pump power. This relationship between the delay and the SBS pump power is found to be linear as well, as shown in $-C5$. The result concludes that the slow-light effect on the signal is transferred successfully to all converted channels through the FWM multicasting process. Here, in Fig. 5(a), we note that the delayed signal exhibits higher OSNR than those of the delayed channels 1 to 5. It is because the power of the SBS amplified signal is much higher than those of the multicast channels, of which the powers are limited by the FWM conversion efficiency. Accordingly, channel 1 is slightly noisier than other channels due to its low conversion efficiency. Furthermore, for each

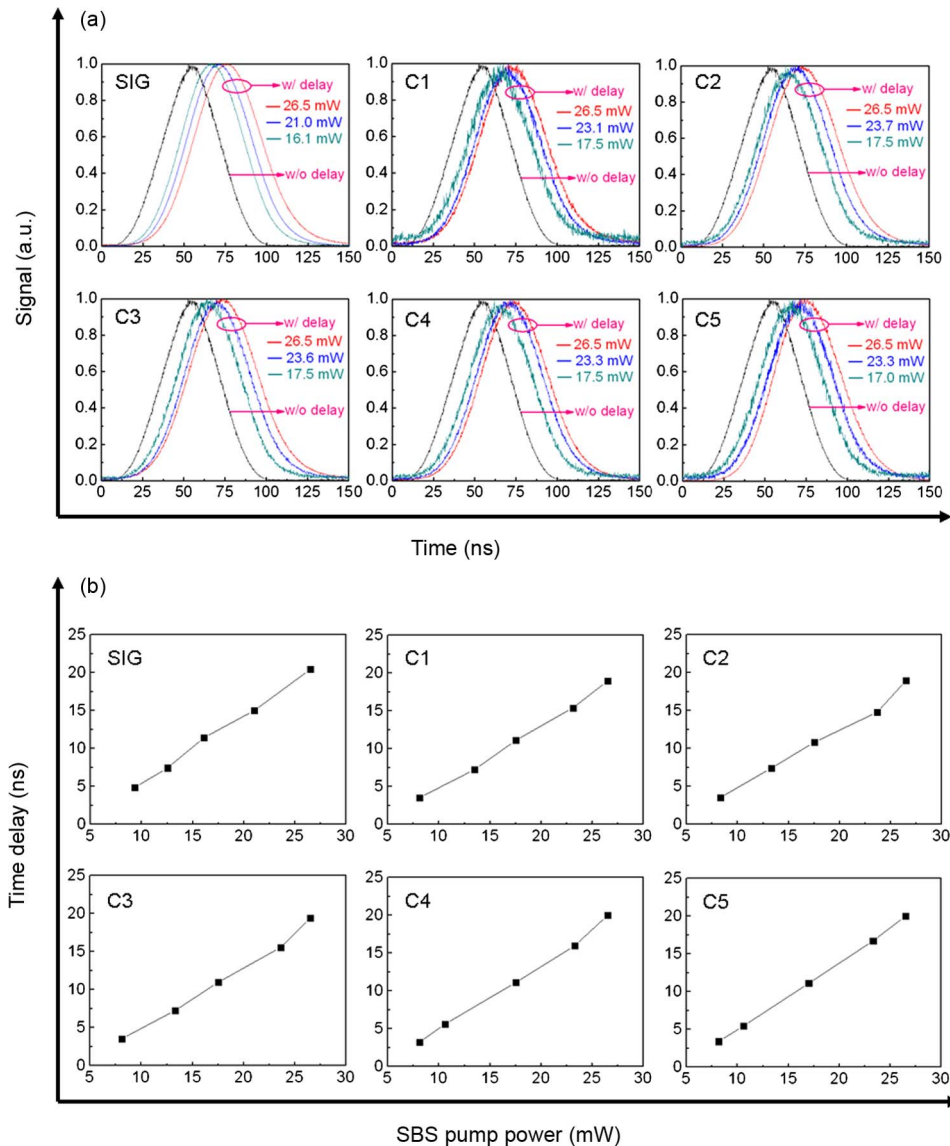


Fig. 5. (a) Measured delayed pulse waveforms for individual channels including the signal and channels 1 to 5 (SIG, C1 to C5) at different SBS pump power levels. Black curves (w/o delay) are for the cases without SBS pump; red, blue, and green curves (w/ delay) are for the cases with SBS pump at different power levels. (b) Time delay versus SBS pump power for individual channels including the signal and channels 1 to 5 (SIG, C1 to C5).

channel including the signal, the OSNR degrades as the SBS pump power is reduced to provide a smaller optical gain. Similar to channel 1, channel 6 exhibits a relatively low conversion efficiency. Hence, we only measure its pulse waveforms at two SBS pump power levels, as depicted in Fig. 6.

From our theoretical analysis, the time delay of the converted channels should be almost the same as that of the delayed signal. To clearly compare their time delays and waveforms, we fix the SBS pump power and tune the center wavelength of the BPF to select each channel in turn for the measurement. The results are plotted in Fig. 7. Fig. 7(c) shows the delayed pulse waveforms of the signal and channels 1 to 5 at three fixed SBS pump power levels: 12.5, 18.3, and 24.4 mW. As mentioned before, the OSNR is smaller at lower SBS pump power levels. Consequently, the delayed pulses in Fig. 7(a) are noisier than those in (b) and (c). At each SBS pump power level, the delayed

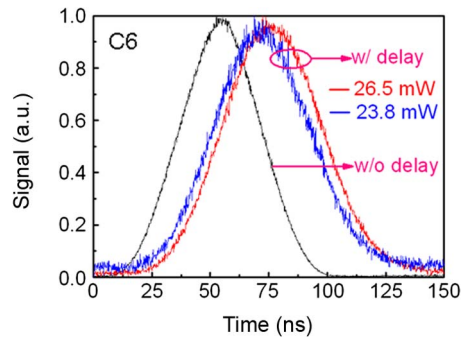


Fig. 6. Measured delayed pulse waveforms for channel 6 at two different SBS pump power levels. The black curve (w/o delay) is for the case without SBS pump; the red and blue curves (w/ delay) are for the cases with SBS pump at different power levels.

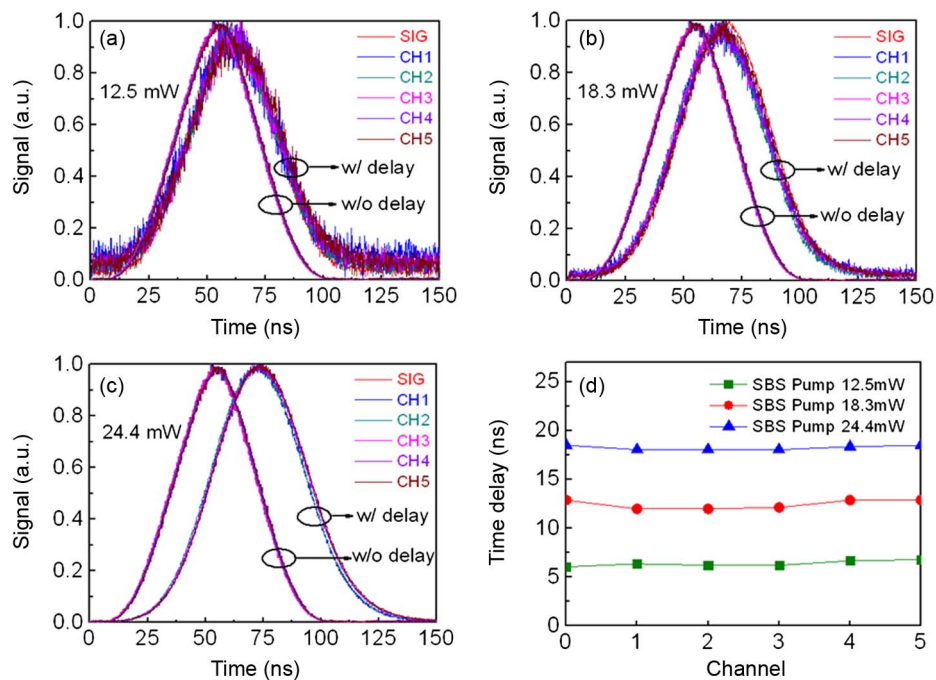


Fig. 7. Measured delayed pulse waveforms from the signal to channel 5 (SIG to CH5) at three fixed SBS pump power levels: (a) 12.5 mW; (b) 18.3 mW; (c) 24.4 mW. The curves labeled “w/o delay” are for the case without SBS pump; the curves labeled “w/ delay” are for the case with SBS pump. (d) Time delay versus channel at three fixed SBS pump power levels; channel 0 is the signal.

pulse waveforms of the converted channels almost overlap completely with that of the signal, implying that they all experience approximately the same time delay. In Fig. 7(d), we show the delays of each channel at the three SBS pump power levels. The average delays at the pump levels are 6.39, 12.47, and 18.27 ns, respectively. The maximum time delay difference among all the channels is 0.89 ns and may be caused by measurement errors and SBS pump power fluctuations.

5. Conclusion

Using FWM wavelength multicast in a single-pump SBS slow-light system, we have demonstrated simultaneous generation of six delayed signals in an HNLF. The time delay performance of the multicasting channels is almost identical to that of the original signal. The maximum delay achieved

is about 20 ns, and the maximum delay difference among the channels is 0.89 ns. To apply the technique for the delay of communication data, one simply needs to enlarge the SBS gain bandwidth by spectral broadening of the SBS pump. This slow-light multicasting technique may find applications in parallel optical information processing such as simultaneous multichannel synchronization and time-division multiplexing.

Acknowledgment

We gratefully acknowledge Finisar in providing a WaveShaper 4000S for the experiment.

References

- [1] A. E. Willner, B. Zhang, L. Zhang, L. Yan, and I. Fazal, "Optical signal processing using tunable delay elements based on slow light," *IEEE J. Sel. Topics Quantum Electron.*, vol. 14, no. 3, pp. 691–705, May 2008.
- [2] L. V. Hau, S. E. Harris, Z. Dutton, and C. H. Behroozi, "Light speed reduction to 17 meters per second in an ultracold atomic gas," *Nature*, vol. 397, pp. 594–598, Feb. 1999.
- [3] M. S. Bigelow, N. N. Lepeshkin, and R. W. Boyd, "Superluminal and slow light propagation in a room-temperature solid," *Science*, vol. 301, no. 5630, pp. 200–202, Jul. 2003.
- [4] M. Notomi, K. Yamada, A. Shinya, J. Takahashi, C. Takahashi, and I. Yokohama, "Extremely large group-velocity dispersion of line-defect waveguides in photonic crystal slabs," *Phys. Rev. Lett.*, vol. 87, no. 25, pp. 253902-1–253902-4, Dec. 2001.
- [5] Y. Okawachi, M. S. Bigelow, J. E. Sharping, Z. Zhu, A. Schweinsberg, D. J. Gauthier, R. W. Boyd, and A. L. Gaeta, "Tunable all-optical delays via Brillouin slow light in an optical fiber," *Phys. Rev. Lett.*, vol. 94, no. 15, pp. 153902-1–153902-3, Apr. 2005.
- [6] K. Y. Song, M. G. Herráez, and L. Thévenaz, "Observation of pulse delaying and advancement in optical fibers using stimulated Brillouin scattering," *Opt. Exp.*, vol. 13, no. 1, pp. 82–88, Jan. 2005.
- [7] M. G. Herráez, K. Y. Song, and L. Thévenaz, "Arbitrary-bandwidth Brillouin slow light in optical fibers," *Opt. Exp.*, vol. 14, no. 4, pp. 1395–1400, Feb. 2006.
- [8] Z. Zhu, A. M. C. Dawes, D. J. Gauthier, L. Zhang, and A. E. Willner, "Broadband SBS slow light in an optical fiber," *J. Lightw. Technol.*, vol. 25, no. 1, pp. 201–206, Jan. 2007.
- [9] A. Cheng, P. Fok, and C. Shu, "Wideband SBS slow light in a single mode fiber using a phase-modulated pump," presented at the Quantum Electronics Laser Science Conf., Baltimore, MA, May 2007, Paper JWA49.
- [10] B. Zhang, L. Zhang, L. Yan, I. Fazal, J. Yang, and A. E. Willner, "Continuously-tunable, bit-rate variable OTDM using broadband SBS slow-light delay line," *Opt. Exp.*, vol. 15, no. 13, pp. 8317–8322, Jun. 2007.
- [11] L. Yi, L. Zhan, W. Hu, and Y. Xia, "Delay of broadband signals using slow light in stimulated Brillouin scattering with phase-modulated pump," *IEEE Photon. Technol. Lett.*, vol. 19, no. 8, pp. 619–621, Apr. 2007.
- [12] B. Zhang, L. Yan, I. Fazal, L. Zhang, A. E. Willner, Z. Zhu, and D. J. Gauthier, "Slow light on Gb/s differential-phase-shift-keying signals," *Opt. Exp.*, vol. 15, no. 4, pp. 1878–1883, Feb. 2007.
- [13] B. Zhang, L. Yan, L. Zhang, S. Nuccio, L. Christen, T. Wu, and A. E. Willner, "Spectrally efficient slow light using multilevel phase-modulated formats," *Opt. Lett.*, vol. 33, no. 1, pp. 55–57, Jan. 2008.
- [14] B. Zhang, L. Yan, J. Yang, I. Fazal, and A. E. Willner, "A single slow-light element for independent delay control and synchronization on multiple Gb/s data channels," *IEEE Photon. Technol. Lett.*, vol. 19, no. 14, pp. 1081–1083, Jul. 2007.
- [15] B. Zhang, L. Yan, L. Zhang, and A. E. Willner, "Multichannel SBS slow light using spectrally sliced incoherent pumping," *J. Lightw. Technol.*, vol. 26, no. 23, pp. 3763–3769, Dec. 2008.
- [16] E. Shumakher, N. Orbach, A. Nevet, D. Dahan, and G. Eisenstein, "On the balance between delay, bandwidth and signal distortion in slow light systems based on stimulated Brillouin scattering in optical fibers," *Opt. Exp.*, vol. 14, no. 13, pp. 5877–5884, Jun. 2006.
- [17] L. Zhang, T. Luo, C. Yu, W. Zhang, and A. E. Willner, "Pattern dependence of data distortion in slow-light elements," *J. Lightw. Technol.*, vol. 25, no. 7, pp. 1754–1760, Jul. 2007.
- [18] T. Schneider, R. Henker, K. Lauterbach, and M. Junker, "Distortion reduction in slow light systems based on stimulated Brillouin scattering," *Opt. Exp.*, vol. 16, no. 11, pp. 8280–8285, May 2008.
- [19] S. Wang, L. Ren, Y. Liu, and Y. Tomita, "Zero-broadening SBS slow light propagation in an optical fiber using two broadband pump beams," *Opt. Exp.*, vol. 16, no. 11, pp. 8067–8076, May 2008.
- [20] S. Chin, M. G. Herráez, and L. Thévenaz, "Complete compensation of pulse broadening in an amplifier-based slow light system using a nonlinear regeneration element," *Opt. Exp.*, vol. 17, no. 24, pp. 21 910–21 917, Nov. 2009.
- [21] A. Wiatrek, K. Jamshidi, R. Henker, S. Preuler, and T. Schneider, "Nonlinear Brillouin based slow-light system for almost distortion-free pulse delay," *J. Opt. Soc. Amer. B*, vol. 27, no. 3, pp. 544–549, Mar. 2010.
- [22] L. Wang, B. Zhou, C. Shu, and S. He, "Stimulated Brillouin scattering slow-light-based fiber-optic temperature sensor," *Opt. Lett.*, vol. 36, no. 3, pp. 427–429, Feb. 2011.
- [23] L. Wang and C. Shu, "Demonstration of distributed strain sensing with the use of stimulated Brillouin scattering-based slow light," *IEEE Photon. J.*, vol. 3, no. 6, pp. 1164–1170, Dec. 2011.
- [24] G. Contestabile, M. Presi, and E. Ciaramella, "A fiber-based 1:6 WDM multicast converter at 10 Gb/s," *Opt. Commun.*, vol. 241, no. 4–6, pp. 499–502, Nov. 2004.
- [25] J. Wang, Q. Sun, and J. Sun, "All-optical 40 Gb/s CSRZ-DPSK logic XOR gate and format conversion using four-wave mixing," *Opt. Exp.*, vol. 17, no. 15, pp. 12 555–12 563, Jul. 2009.

- [26] J. Wang, S. R. Nuccio, J. Yang, X. Wu, A. Bogoni, and A. E. Willner, "High-speed addition/subtraction/complement/doubling of quaternary numbers using optical nonlinearities and DQPSK signals," *Opt. Lett.*, vol. 37, no. 7, pp. 1139–1141, Apr. 2012.
- [27] Y. Dai and C. Shu, "Polarization insensitive wavelength multicasting of DPSK signal using four-wave mixing in a birefringent photonic crystal fiber," *Opt. Commun.*, vol. 285, no. 16, pp. 3545–3548, Jul. 2012.
- [28] J. Liu, T. Cheng, Y. Yeo, Y. Wang, L. Xue, W. Rong, L. Zhou, G. Xiao, D. Wang, and X. Yu, "Stimulate Brillouin scattering based broadband tunable slow-light conversion in a highly nonlinear photonic crystal fiber," *J. Lightw. Technol.*, vol. 27, no. 10, pp. 1279–1285, May 2009.
- [29] N. Shibata, R. P. Braun, and R. G. Waarts, "Phase-mismatch dependence of efficiency of wave generation through four-wave mixing in a single-mode optical fiber," *IEEE J. Quantum Electron.*, vol. 23, no. 7, pp. 1205–1210, Jul. 1987.
- [30] G. P. Agrawal, *Nonlinear Fiber Optics*, 4th ed. Amsterdam, The Netherlands: Elsevier, 2009.
- [31] E. Mateo, F. Yaman, and G. Li, "Control of four-wave mixing phase-matching condition using the Brillouin slow-light effect in fibers," *Opt. Lett.*, vol. 33, no. 5, pp. 390–488, Mar. 2008.